Available online at www.sciencedirect.com

ScienceDirect

JOURNAL OF IRON AND STEEL RESEARCH, INTERNATIONAL. 2013, 20(1): 62-70

Structural Ultrafine Grained Steels Obtained by Advanced Controlled Rolling

R González[1], J O García[2], M A Barbés[2], M J Quintana[1], L F Verdeja[2], J I Verdeja[2]

(1. School of Engineering, Panamerican University, Mexico City 03920, Mexico;
2. E T S I M O, Oviedo University, Oviedo 33004, Spain)

Abstract: Steels with ultrafine grains (lower than 5 μm), which usually known as ultrafine ferrite or ultrafine grained materials, are presently the object of intense research, because of the improvement in resistance and fracture toughness they may reach compared to conventional steels (with grain sizes above this value). It is shown that the fore-named steels designated in the Euronorm EN 10149-2, which are manufactured by advanced techniques of controlled rolling and mainly used in automotive industry, have an ultrafine grain size in the range of 2.5 to 3.5 μm, and with elastic yield stresses higher than 400 MPa. Based on the Morrison-Miller criterion, it is shown that values of the strain-hardening coefficient lower than 0.08 would make the industrial application of these steels unfeasible.

Key words: ultrafine grained steel; mechanical property; manufacturability; strain-hardening

In recent years an increasing interest has been developed in both industrial and laboratory levels, for the production of non-alloyed, low-alloyed and micro-alloyed steels with ultrafine grains defining these steels as those with ASTM G grain size higher than 12 (5 μm or less)[1-2]. A higher resistance and fracture toughness at temperatures below 0 ℃ is expected from this new generation of steels. Two tendencies appear as fundamental: laboratories dedicated to scientific research and not connected to the steelmaking industry, which pursue this objective using techniques that involve large deformations (SPD process: severe plastic deformation) with deformations $\varepsilon = 4$, and those laboratories directly inside or linked to the industrial process—which is the case of the Sid-met-mat group of ETSIMO (Spain)—that use advanced technologies in thermomechanical controlled rolling processes (ATMCRP) and propose an alternative in the mass production of ultrafine ferrite (UFF) or ultrafine grained (UFG) steels. This is possible[3] due to recent advancements in the steelmaking industry: improvements in both information technologies and process automation have allowed the crossover from laboratory to industrial level of UFG steels, now commonly used (particularly in the automotive sector).

The present work shows that steels specified in Euronorm EN 10149-2 are in fact UFF steels which ArcelorMittal de Asturias (Spain) produced 305 000 t of hot rolled structural strip steels in 2010, and from those, 60 000 t were delivered in raw hot-rolled conditions in different specifications indicated by the Euronorm.

1 Experimental Work and Results

This work contemplates four steels included in the Euronorm and detailed in Table 1 and Table 2: S315, S420, S500 and S600, respectively alloyed with Nb or Nb/Ti, in the form of steel sheet and with thickness below or equal to 5 mm obtained by ATMCRP (hot-rolled raw state) in the factory of ArcelorMittal in Avilés (Oviedo, Spain). This process consists in the control of the speed and amount of deformation of sheets at adequate times and temperatures to achieve the UFG microstructure, in the following steps.

1) Homogenization. The slabs obtained by continuous casting (approximately 230 mm×1 580 mm×7 120 mm) are maintained at temperatures of 1 200－1 250 ℃ to start with a recrystallized structure.

2) Roughing. In reversible rolling trains (husk tool and roughing tool), approximately 10 passes (with

Biography: R González(1967—), Male, Doctor; **E-mail**: robglez@up.edu.mx; **Received Date**: March 11, 2011

Table 1 Chemical composition of thermomechanically rolled steels (mass percent, %)

Name	Material number	C	Mn	Si	P	S[1)]	Al_t	Nb[2)]	V[2)]	Ti[2)]	Mo	B
S315	1.0972	≤0.12	≤1.30	≤0.50	≤0.025	≤0.020	≥0.015	≤0.09	≤0.20	≤0.15	—	—
S355	1.0976	≤0.12	≤1.50	≤0.50	≤0.025	≤0.020	≥0.015	≤0.09	≤0.20	≤0.15	—	—
S420	1.0980	≤0.12	≤1.60	≤0.50	≤0.025	≤0.015	≥0.015	≤0.09	≤0.20	≤0.15	—	—
S460	1.0982	≤0.12	≤1.60	≤0.50	≤0.025	≤0.015	≥0.015	≤0.09	≤0.20	≤0.15	—	—
S500	1.0984	≤0.12	≤1.70	≤0.50	≤0.025	≤0.015	≥0.015	≤0.09	≤0.20	≤0.15	—	—
S550	1.0986	≤0.12	≤1.80	≤0.50	≤0.025	≤0.015	≥0.015	≤0.09	≤0.20	≤0.15	—	—
S600	1.8969	≤0.12	≤1.90	≤0.50	≤0.025	≤0.015	≥0.015	≤0.09	≤0.20	≤0.22	≤0.50	≤0.005
S650	1.8976	≤0.12	≤2.00	≤0.60	≤0.025	≤0.015	≥0.015	≤0.09	≤0.20	≤0.22	≤0.50	≤0.005
S700	1.8974	≤0.12	≤2.10	≤0.60	≤0.025	≤0.015	≥0.015	≤0.09	≤0.20	≤0.22	≤0.50	≤0.005

Note: 1) If ordered, the maximum sulphur content shall be 0.01%; 2) The sum of Nb, V and Ti shall be no more than 0.22%.

Table 2 Mechanical properties for thermomechanically rolled steels

Name	Material number	Minimum yield strength/MPa	Tensile strength/MPa	Minimum percentage elongation at fracture		Bending force at 180° minimum mandrel diameter/N
				If $t<3$ $L_0=80$ mm	If $t\geqslant 3$ $L_0=5.65\sqrt{S_0}$	
S315	1.0972	315	390—510	20	24	0
S355	1.0976	355	430—550	19	23	0.5
S420	1.0980	420	480—620	16	19	0.5
S460	1.0982	460	520—670	14	17	1.0
S500	1.0984	500	550—700	12	14	1.0
S550	1.0986	550	600—760	12	14	1.5
S600	1.8969	600	650—820	11	13	1.5
S650	1.8976	650	700—880	10	12	2.0
S700	1.8974	700	750—950	10	12	2.0

Note: 1) The values for the tensile test apply to longitudinal test pieces. The values for the bent test apply to transverse test pieces. For thickness $t>8$ mm, minimum yield strength can be lower than 20 MPa; 2) L_0 is the initial length of the tension test sample; 3) S_0 is the initial width of the tension test sample.

rolling speeds between 2—3.25 m/s) are made to reduce the thickness to about 40 mm (approximately 20 mm per pass) and maintain at a temperature of 1200—1100 ℃.

3) Waiting. Before the finishing train, the material is cooled to 1100—1000 ℃.

4) Finishing. Consist in a train of hot or semicontinuous bands (7 boxes). The temperature drops to 850 ℃, and a thickness of about 5 mm is obtained.

5) Controlled cooling. Atomized water is used as a cooling method until it reaches coiling temperature (about 600 ℃).

6) Coiling. The sheet is coiled at a temperature of about 600 ℃. It is very important that the coiling cooling rate results in a ferritic-pearlitic ultrafine structure.

The laboratory chemical analysis (Table 3), performed on two samples for each steel, included the following items: C and S were analyzed by combustion in a LECO CS-200 equipment; the remaining elements by optical emission spectrometry in an ARL 3460 system. As expected from the Euronorm specification and manufacturing process, S500 and S600 are microalloyed with Nb/Ti and high Mn within the specification range.

Tension testing was made in longitudinal samples extracted from the steel sheet, with calibrated length L_0 in accordance to EN 10002-1 standard. The equipment used was an INSTRON 5583 machine, with a 150 kN capacity load cell, specially adapted for

Table 3 Chemical analysis of four steel samples tested (mass percent, %)

Sample	C	Mn	Si	S	P	Ti	Nb	Al
S315	0.07	0.33	0.01	0.013	0.008	—	0.023	0.042
S420	0.10	0.47	0.01	0.010	0.016	—	0.044	0.029
S500	0.09	1.41	0.02	0.012	0.019	0.075	0.047	0.031
S600	0.09	1.45	0.02	0.008	0.019	0.074	0.047	0.026

tension testing of either hot or cold rolled plane products. The parameters evaluated (Table 4) were higher yield stress, lower yield stress, yield elongation, rupture stress, elongation before rupture, lower yield/rupture stress ratio and strain hardening coefficient n. All the steels comply with the specifications of the EN 10149-2 standard, with the exception of the S600 yield stress which is at the limit of the specification. Engineering stress-strain curves for the samples are presented in Fig. 1, and for comparison, the ones for ULC steel (C 0.003%, Mn 0.15% and Ti 0.07%) indicated as IF and with extra-deep-drawing quality ($n=0.25$) and a dual phase steel (C 0.1%, Si 0.55%, Mn 1.6% and B 0.005%) indicated as DP with commercial quality ($n=0.22$) are given.

Table 4 Mechanical properties and quantitative metallographic results

Property	S315 sample	S420 sample	S500 sample	S600 sample
Thickness/mm	4.0	5.2	4.5	2.3
Higher yield stress/MPa	369	465	630	585
Lower yield stress/MPa	357	449	618	581
Yield elongation/%	0.5	2.0	2.3	0.6
Rupture stress/MPa	421	534	678	661
Elongation before rupture/%	20	27	26	16
Lower yield/rupture stress ratio	0.85	0.84	0.91	0.88
Strain hardening coefficient	0.19	0.16	0.10	0.10
$\overline{G}$(ASTM)	13.0	13.3	14.2	13.9
σ_G(ASTM)	1.50	1.47	1.05	1.20
$\overline{L}/\mu m$	3.50	3.10	2.30	2.50

Note: 1) $\overline{G}$ is the mean ASTM grain size number; 2) σ_G is the standard deviation of the ASTM grain size distribution; 3) $\overline{L}$ is the mean linear intercept grain size.

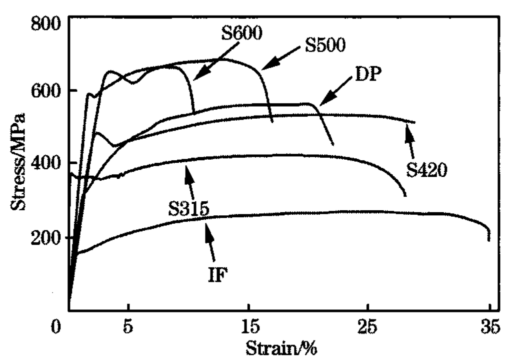

Fig. 1 Engineering tensile curves for investigated steels

Metallographic analysis was carried out in the transverse section of the steel sheet parallel to the rolling direction, followed by mechanical grinding, 6 and 1 μm diamond paste polishing and using a 0.05 μm γ-alumina solution to achieve mirror finish. The etching solution to reveal microstructures was Nital-2, a 2% nitric acid solution in alcohol. Quantitative metallography was made using a Nikon-Epiphot equipment, and because these are UFF steels, to evaluate the ASTM G grain size, optical objectives M_s higher than 100 magnification were used, just as recommended by the ASTM E-112 standard. The formula[4]

$$G=G'+6.64\lg\left(\frac{M_s}{100}\right) \tag{1}$$

was used to convert grain size. To quantitatively determine the statistical distribution of grain sizes (mean linear intercept $\overline{L}$), a Buehler Omnimet image analyzer connected to the Nikon-Epiphot microscope was used, in accordance to the already quoted E 112 standard, and to the extended E 1181-02 version.

The intercept measurements are automatically made by the equipment with lines traced over the micrograph at 0°, 45°, 90° and 135° of the rolling direction. The distribution of grain sizes (histogram) follows a log-normal law. The relation between ASTM G number and linear intercept sizes is:

$$G=-3.356-6.644\lg\overline{L} \tag{2}$$

The statistical distribution of frequency versus G size is of the normal type. Thus, the mean grain size G and standard deviation σ_G were determined using 6 micrographs for each steel and reporting the average value and standard deviation (Table 4). The values indicate (Fig. 2 to Fig. 5) that these are in fact UFF steels with mean grain size values in the range of 13–14 ASTM (3.5–2.5 μm).

The optical micrographs of these steels have the following common characteristics.

1) Slight banding of the ferrite-pearlite structure in the rolling direction, where the volume fraction of pearlite is also quantitatively analyzed, never surpasses 5%, therefore making the structure, from a mechanical point of view, as single phase.

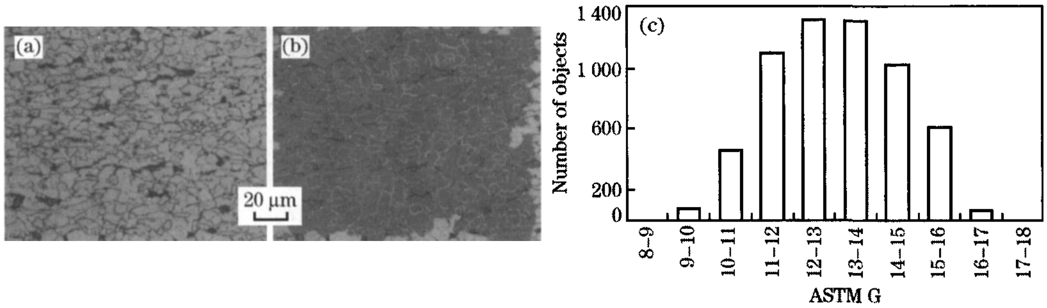

Fig. 2 Metallographic image sample S315 (a), along with detected grain pattern (b) and ASTM G grain size distribution histogram (c)

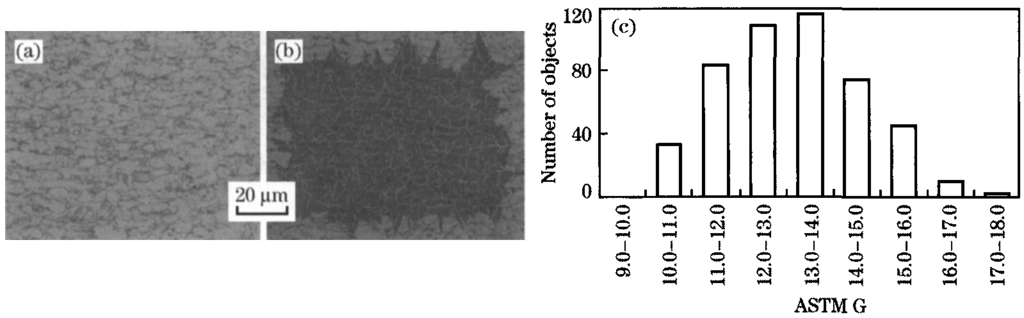

Fig. 3 Metallographic image sample S420 (a), along with detected grain pattern (b) and ASTM G grain size distribution histogram (c)

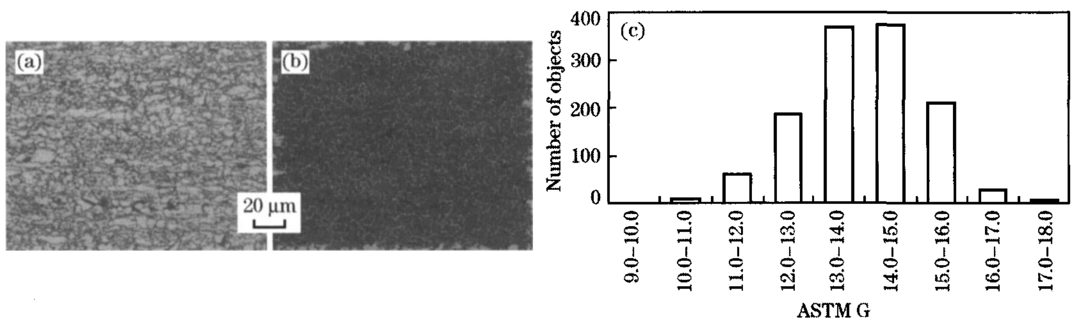

Fig. 4 Metallographic image sample S500 (a), along with detected grain pattern (b) and ASTM G grain size distribution histogram (c)

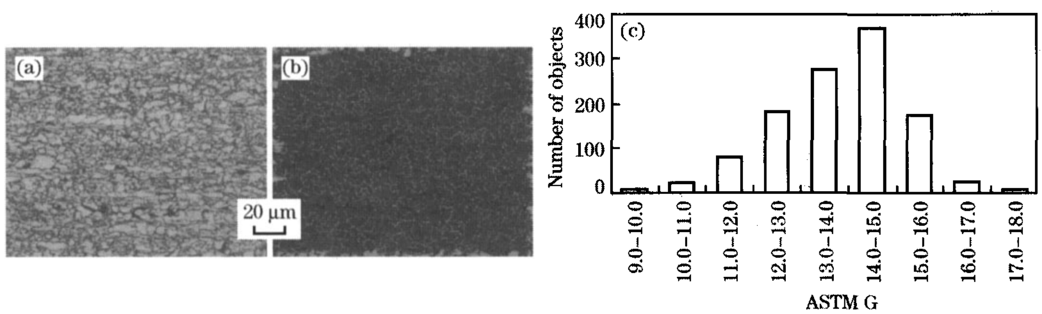

Fig. 5 Metallographic image sample S600 (a), along with detected grain pattern (b) and ASTM G grain size distribution histogram (c)

2) "Pancake" structure of the ferrite phase inherits from the controlled rolling process, with elongated grains in the rolling direction, which makes indispensable, as indicated before, to measure intercepts in lines with different angles to obtain a correct $\overline{L}$ value.

3) The structures are recrystallized, though no evidence of sub-grains was found, typical in restored states.

2 Discussion

As already indicated, the works published in the last decade on UFF steels are abundant, using different technologies, all of them developed until now in a laboratory level, with examples such as:

1) Hot-rolling processes, followed by large deformations in warm temperature and rapid cooling developed at the Max Planck Institute (Germany), producing grain sizes close to 1.6 μm[5].

2) Dynamic Strain Induced Transformation (DSIT) processes of hot-rolled sheets performed at Deakin University, Australia, with large deformations ($\varepsilon \approx 3$) in the $A_3 - A_{r3}$ interval, followed by controlled cooling, reaching grain sizes close to 0.5 μm[6-7].

3) Severe Plastic Deformation (SPD) and Accumulative Roll Bonding (ARB) on steel and aluminum sheets at the Universities at Osaka and Tokyo, Japan, subjected to various cycles of deformation (cumulative deformation $\varepsilon_t \approx 5$) and subcritical annealing. Grain sizes of 0.2 μm may be reached[8-10]

4) Rapid Transformation Annealing (RTA) processes which consist in large cold reductions of thickness in steel sheets ($1<\varepsilon<3$), followed by flash-annealing (lasting a few seconds) at subcritical ($<A_{c1}$), intercritical ($A_{c1}<T<A_{c3}$) or complete austenization temperatures. The University of Aachen, Germany, and CEIT de Guipuzcoa, Spain, have obtained grain sizes with values of 2 to 3 μm[11]. Similar procedures have been used in the Research and Development Division of Tata Steel (India), working with low carbon martensitic steels[12].

All the research groups just mentioned have found what A A Howe[13], very wisely, has defined as the Achilles' heel of the UFF materials: there is an inferior limit for the grain size of these steels below which they are not able to homogenously strain-harden and are, therefore, unviable for processes of drawing and/or expansion cold-forming. The demonstration of this, is based on the works of W B Morrison et al[14-15] and focuses on the n coefficient of strain hardening, quoted in texts on metallic materials[16-23], and its correlation to grain size. In a resumed way, the argument is the following: when tested in tension, ductile materials—such as steel—show a response in the uniform deformation plastic zone that fits a Ludwik-Hollomon law type:

$$\sigma = K\varepsilon^n \tag{3}$$

where, σ is the true tension stress; ε is the true strain; K is a proportional constant and n is the strain hardening coefficient.

Fig. 6 presents the s_y/K value plotted versus ε for the investigated steels. On the other hand, ductile materials (steels included) also show a relation—based on deformation by dislocation movement—between yield stress s_y and grain size, consistent with the Hall-Petch formula:

$$s_y = s_0 + kd^{-1/2} \tag{4}$$

where, s_y is the engineering lower yield stress; s_0 is the Peierls tension or resistance of the crystal lattice to the movement of dislocations; k is a constant function of the chemical composition of the steel and d is the grain size, usually expressed in mm.

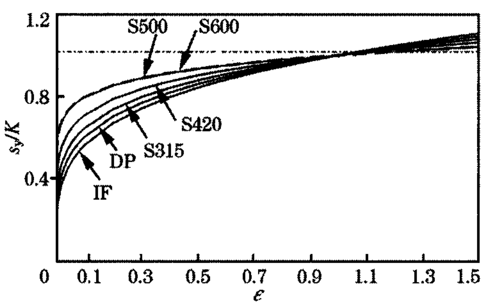

Fig. 6 s_y/K **as a function of** ε

There are numerous theories (and formulas) to correlate composition, structure and mechanical properties of low, medium and high carbon steels, as well as stainless steels[17,19,23-24], and all of them were considered as the starting point of the Hall-Petch law and used linear regression multivariable methods: a relation is established between the yield stress s_y and the inverse square root of grain size. This law may also be applied to the fracture stress s_u and to the Charpy (or Izod) transition temperature (ITT). Both of them are very important in the design and application of structural steels, as the following examples show.

1) According to F B Pickering[17] for low carbon, ferritic-pearlitic, weldable steels, the formulas may be:

$$s_y = 54 + 32w_{Mn} + 83w_{Si} + 354w_{N_f} + 17d^{-1/2} \tag{5}$$

$$s_u = 295 + 28w_{Mn} + 83w_{Si} + 4w_{pear} + 8d^{-1/2} \tag{6}$$

where, w_{Mn}, w_{Si}, w_{N_f} and w_{pear} are the mass percent of alloying elements Mn, Si, frce N and pearlite. Not considering (as a first approximation) the influence of alloying elements:

① 0% pearlite steel (pure ferrite) as in an interstitial free (IF) steel

$$s_y \approx 54 + 17d^{-1/2} \tag{7}$$

$$s_u \approx 295 + 8d^{-1/2} \tag{8}$$

$$s_y = s_u \rightarrow d^{-1/2} = 26.8 \rightarrow d = 1.4 \tag{9}$$

Substituting in Eqn. (7) and Eqn. (8):

$$s_y = s_u \approx 510 \quad (10)$$

② 15% pearlite steel (about 0.1% C) as in low-carbon mild steel

$$s_y = s_u \to d^{-1/2} \approx 33.4 \to d = 0.9 \quad (11)$$

$$s_y = s_u \approx 620 \quad (12)$$

③ 25% pearlite steel (about 0.2% C) as in structural steel

$$s_y = s_u \to d^{-1/2} \approx 37.9 \to d = 0.7 \quad (13)$$

$$s_y = s_u \approx 700 \quad (14)$$

If s_y (and s_u) are plotted against $d^{-1/2}$ or d, it follows that the minimum grain size (critical size) that cancels the ductility of the steel is close to 1 μm.

2) According to D T Gawne and G M H Lewis[24] the correlations would be

$$s_y = 27 + 22d^{-1/2} + 165w_C + 470w_P + 3\,000w_{N_f} + 60w_{Si} - 665w_S \quad (15)$$

$$s_u = 150 + 16d^{-1/2} + 335w_C + 600w_P + 4\,505w_{N_f} + 77w_{Si} - 845w_S \quad (16)$$

with the numbers expressed in the same way as Eqn. (5) and Eqn. (6). Using the same assumptions as in the previous case:

① 0% pearlite steel (pure ferrite) as in a IF steel

$$s_y \approx 27 + 22d^{-1/2} \quad (17)$$

$$s_u \approx 150 + 16d^{-1/2} \quad (18)$$

$$s_y = s_u \to d^{-1/2} = 20.5 \to d = 2.4 \quad (19)$$

Substituting in Eqn. (15) and Eqn. (16):

$$s_y = s_u \approx 480 \quad (20)$$

② 15% pearlite steel (about 0.1% C) as in low-carbon mild steel

$$s_y = s_u \to d^{-1/2} \approx 23.7 \to d = 1.8 \quad (21)$$

$$s_y = s_u \approx 565 \quad (22)$$

③ 25% pearlite steel (about 0.2% C) as in structural steel

$$s_y = s_u \to d^{-1/2} \approx 26.83 \to d = 1.4 \quad (23)$$

$$s_y = s_u \approx 650 \quad (24)$$

In other words, the resulting critical grain sizes are above 1 μm and, therefore, mechanical resistances are lower than those predicted by F B Pickering[17]. In any case, both works agree in a ferrite critical grain size of about 1 μm that will annul ductility. A 2.5 μm grain size (ASTM 14) would be a more conservative value, and in this case, the presence of a hardening phase (pearlite) diminishes the critical grain size. These two conclusions are very important in the process of designing UFF steels.

By accepting Eqn. (3) and Eqn. (6), it may also be deduced the existence of a functional relation between n and d, known as the Morrison law[14]:

$$n = 5/(10 + d^{-1/2}) \quad (25)$$

This formula, which establishes an inverse proportional relation between n and d, is particularly relevant for UFF (UFG) steels.

Steels that present a tensile curve with a higher yield stress, lower yield stress and yield elongation by propagation of Lüders bands (plastic instability prior to uniform deformation), of ε_L value (true Lüders strain), may loose their capacity for homogenous deformation if the following condition[15] is verified:

$$\varepsilon_L = n \quad (26)$$

Therefore, non-homogenous Lüders deformations eliminate the capacity for strain hardening of the steel. Applying Eqn. (3) and Eqn. (26) and relationships between engineering and true stress, it follows that:

$$s_y(1 + e_L) = K\varepsilon_L^n \quad (27)$$

where, taking logarithms in both sides of the equation and regrouping, leads to the expression:

$$\ln \frac{K}{s_y} = \varepsilon_L - n\ln\varepsilon_L = n(1 - \ln n) \quad (28)$$

Fig. 7 presents the analytical expression for this last formula, where the limit curve, which corresponds to the $\varepsilon_L = n$ criterion is plotted, and separates the upper part of stable steels ($n > \varepsilon_L$) from the unstable ones ($n < \varepsilon_L$). The first ones overpass the yield elongation and strain hardening, while the second ones ($n \leqslant \varepsilon_L$) fail to accomplish these aspects. In the figure, the UFF steels investigated in this work are presented, along with the reference DP and IF steels, all of them in the stable plastic deformation zone.

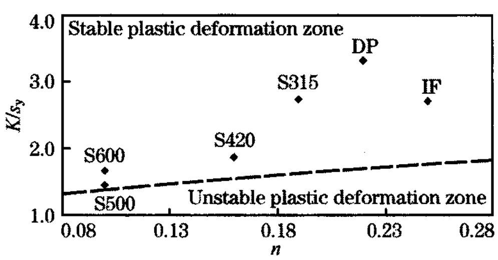

Fig. 7 K/s_y in accordance to Eqn. (28)

From these considerations it may be deduced that there is a "natural" inferior limit imposed to UFG steels and their corresponding grain size d and homogenous deformation n, utterly connected to the deformation by dislocation movement and pile-up strengthening behavior[18]. In all cases the n coefficient should be higher than 0.08 (as may be seen in Fig. 8). For $n = 0.1$, the Morrison law [Eqn. (25)] requires a 0.6 μm grain size that seems excessively small, though, as reported by N Tsuji et al[8] in an exhaustive work carried out on commercial aluminum alloys (1100 grades) and ULC IF steels ($w_C <$ 0.003%, microalloyed with Ti), the critical grain size in these materials is close to 1 μm, beneath which the yield stress and tensile stress match up, making uniform deformation impossible, at least at room temperature. Fig. 9 presents both the ASTM G grain size (on the left) and the mean linear intercept $\overline{L}$ in μm (on the right) as a function of the n coefficient for the four steels investigated. In the case of $\overline{L}$ (lower part of the figure) a second-degree-fit curve indicates a value below 2 μm for $n=0.08$ coefficient limit ($s_y/s_u \approx 1$ in Fig. 8). In a similar way (upper part of the figure), the ASTM G grain size is shown, along with the upper and lower limits for a 95% confidence level of these measurements. The second-degree-fit curves indicate that for an n value of 0.08, the corresponding mean grain size is close to 14.

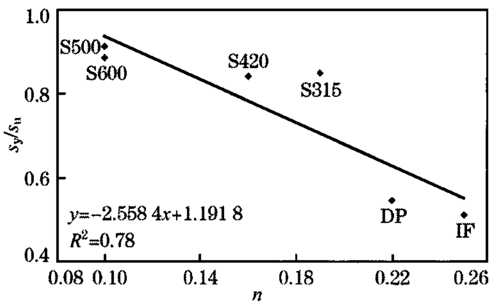

Fig. 8 s_y/s_u **as a function of** n

To conclude, as there is a correlation between the value of the s_y/s_u ratio and the n coefficient (as shown in Fig. 8) there is a minimum value $n \approx 0.08$ for which s_y/s_u has a value lower than 1 and a threshold for uniform plastic deformations. Thus, microalloyed UFF ferrite-pearlite steels obtained by AT-MCRP may reach 600 MPa in yield stress with limit values of $n \approx 0.1$ and $d \approx 2.5$. Increasing the yield stress over 600 MPa (S650 and S700 steels of the EN 10149-2 standard) would imply a raise in the Mn content, addition of Mo and microalloying B (besides Ti/Nb). These steels after controlled rolling and rapid cooling will present in the hot rolling raw state, ferritic-pearlitic-bainitic-martensitic structures: they are dual and multi-phase steels with ultrafine grain sizes below 2 μm. The work "Fundamentals of Dual-Phase steels"[25] explains the possibilities of strain hardening and cold work manufacturing on these materials, product of the increase in the n coefficient[26]. These dual-phase steels are a new class of high-strength low alloy (HSLA) materials characterized by a microstructure consisting of a dispersion of about 20%-30% of hard martensite islands in a soft, ductile ferrite matrix, although small amounts of bainite, pearlite, and retained austenite may also be presented. These steels have a number of unique properties (sometimes called multi-phase properties), which include:

1) Continuous yielding behavior (no yield point and Lüdering elongation);

2) A low 0.2% offset yield strength (≈300 MPa);

3) A high tensile strength (≈600 MPa);

4) A high work hardening rate;

5) An unusually high uniform and total elongation. The high work-hardening rate results in a yield strength of 500 MPa after only 5%-10% deformation.

As a result, in formed parts dual-phase steels have a yield strength comparable to that of other 600 MPa

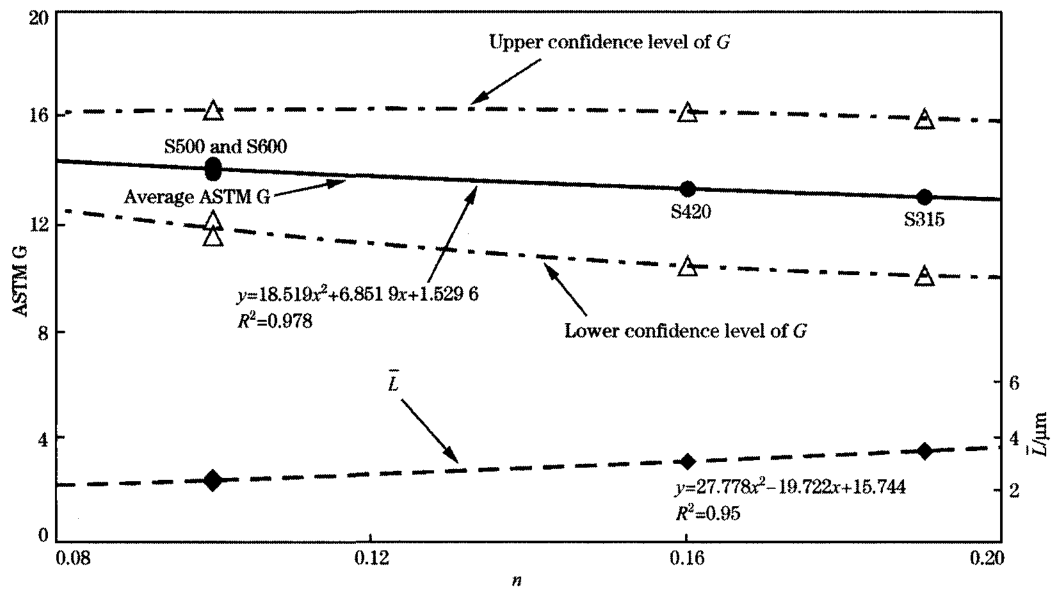

Fig. 9 $\overline{L}$ **and** G **as a function of** n **for four ultrafine grained steels investigated**

HSLA steels (S600) and much better ductility. More importantly, the high work-hardening rate, combined with the high uniform elongation of these steels, gives them a formability equivalent in stretching to that of much lower strength sheet steels (deep-drawing quality and drawing-quality). As a result these steels are an attractive material for weight-saving applications in automobiles.

Dual-phase steels can be produced either in the hot-rolled state (S650 and S700) or by intercritical heat treatment with either continuous annealing or box annealing technologies. Actual production has concentrated on using continuous-annealing processing lines because of higher production rates, better uniformity of properties, and the possibility to use lower alloy steels[26-27].

Fig. 10 and Fig. 11 show the micrographs, ASTM grain size distributions and presence of ferrite and martensite, respectively in a DP600 (in hot rolled state as demanded by RUR Group) steel, which has been used as a reference in this work. This material is also an ultrafine grained steel, and the reason for its low s_y/s_u ratio (high ductility) is the residual stresses introduced by the austenite during the martensitic transformation, after cooling into a ferritic matrix. In other words, the transformation occurs at low temperature (below 500 ℃) causing the ferritic phase to withstand the volume expansion (2% − 4%). As a result, both a high dislocation density and residual stresses are generated at the ferritic phase surrounding martensite. In a simplified interpretation of the phenomena, the deformation pattern takes the form of thin bands of alternated deformed and not-deformed regions, parallel to the rolling direction. This pattern causes continuous yielding, which is a consequence of its yielding nucleation at many points in the sheet[19,21,25]. This mechanical behaviour is similar to pre- and post-tensioned steel reinforced concrete: steel bars work in tension (like ferrite) and bainite and martensite in compression (like concrete), increasing ductility and delaying fracture of the composite.

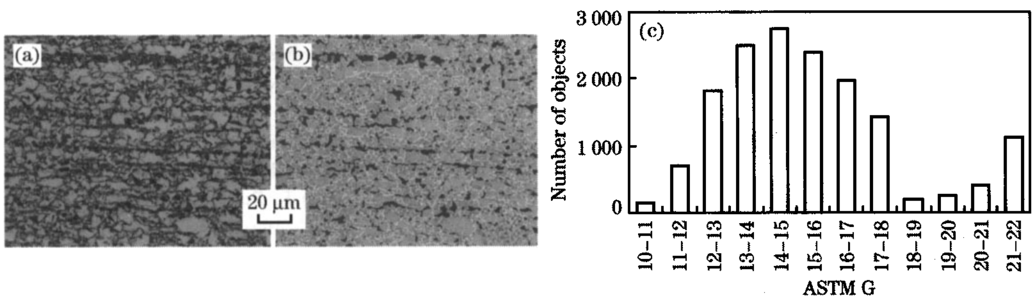

Fig. 10 Metallographic image sample DP showing ferrite (a), along with detected grain pattern (b) and ASTM G grain size distribution histogram (c)

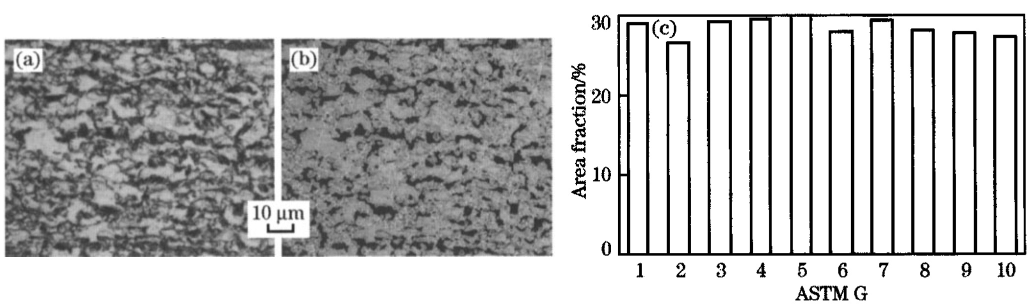

Fig. 11 Metallographic image sample DP showing martensite (a), along with detected grain pattern (b) and martensite volume (measured by area) fraction histogram (c)

3 Conclusions

Low C steels microalloyed with Nb/Ti and ferritic-pearlitic structures standardized by EN 10149-2, manufactured by ATMCRP in the ArcelorMittal de Asturias (Spain) factories are mainly used in automotive applications (fittings and reinforcement parts).

Denominations S315 to S600 investigated in this work have grain sizes lower than 5 μm (ASTM 12) and may be classified as UFF steels. Grain size is mainly in the ASTM 13−14 (3.5 to 2.5 μm) interval.

The strain hardening coefficient n is, in all cases, higher than 0.1, which makes them suitable for not-too-demanding cold work (bending and drawing), as indicated by the mentioned Euronorm.

If an excessive grain size refinement (reaching values close to 1 μm) results in a coefficient n value lower than 0.08, the steel would be plastically unstable (Lüders deformations): strain hardening would be impossible and the material industrially (in practice) unacceptable.

Microalloyed ferritic-pearlitic ultrafine grained steels with yield stresses higher than 600 MPa (including dual and multiphase steels), slightly alloyed with Mn/Mo, microalloyed with Ti/Nb/B and manufactured by ATMCRP, present second phases of the bainitic-martensitic type and reach values of $n>0.1$, and thus, higher than the critical value of $n=0.08$.

The authors wish to thank the Research and Hot Coil Products Department of the ArcelorMittal in Asturias (Spain) Factories (formerly Ensidesa, CSI Planos, Aceralia and Arcelor). They also acknowledge Ms Teresa Iglesias and Ms Bertha Mendieta for their invaluable help in experimental work and text and figures revisions.

References:

[1] Tadashi Furuhara. Special Issue on Ultrafine Grained Steels [M]. Japan: ISIJ International, 2008.
[2] González R, García J O, Barbés M A, et al. Ultrafine Grained HSLA Steels for Cold Forming [J]. Journal of Iron and Steel Research International, 2010, 17(10): 50.
[3] Eager T. The Quiet Revolution in Materials Manufacturing and Production [J]. Journal of Metals, 1998, 50(4): 19.
[4] Vander Voort, Metallography G F. Principles and Practice [M]. Ohio: ASM International, 1999.
[5] Morris P, Beynon J, Ridal K. Advances in the Hot Rolling of Steels [J]. Ironmaking and Steelmaking, 2004, 31(1): 8.
[6] Beladi H, Kelly G L, Hodgson P D. The Effect of Multiple Deformations on the Formation of Ultrafine Grained Steels [J]. Metallurgical and Materials Transactions, 2007, 38A (3): 450.
[7] Beladi H, Kelly G L, Hodgson P D. Ultrafine Grained Structure Formation in Steels Using Dynamic Strain Induced Transformation Processing [J]. International Material Review, 2007, 52(1): 14.
[8] Tsuji N, Ito I, Saito Y, et al. Strength and Ductility of Ultrafine Grained Aluminum and Iron Produced by ARB and Annealing [J]. Scripta Materialia, 2002, 47(12): 893.
[9] Sakai T, Belyakov A, Miura H. Ultrafine Grain Formation in Ferritic Stainless Steel During Severe Plastic Deformation [J]. Metallurgical and Materials Transactions, 2008, 39A (9): 2206.
[10] Okitsu Y, Takata N, Tsuji N. A New Route to Fabricate Ultrafine Grained Structures in Carbon Steels Without Severe Plastic Deformation [J]. Scripta Materialia, 2009, 60(2): 76.
[11] Lesch C, Alvarez P, Bleck W, et al. Rapid Transformation Annealing: A Novel Method for Grain Refinement of Cold-Rolled Low-Carbon Steels [J]. Metallurgical and Material Transactions, 2007, 38A(9): 1882.
[12] Ghosh C, Haldar A, Ghosh P, et al. Microstructure, Texture, Grain Boundary Characteristics and Mechanical Properties of a Cold Rolled and Annealed Martensitic Steel [J]. ISIJ International, 2008, 48(11): 1626.
[13] Howe A A. Ultrafine Grained Steels: Industrial Prospects [J]. Materials Science and Technology, 2000, 16(11/12): 1264.
[14] Morrison W B. The Effect of Grain Size on the Stress-Strain Relationship in Low-Carbon Steel [J]. Transactions of the ASM, 1966, 59: 824.
[15] Morrison W B, Miller R L. The Ductility of Ultra-Fine-Grain Alloys. Ultrafine-Grain Metals [M]. NY, USA: Syracuse University Press, 1970.
[16] Backofen W A. Deformation Processing [J]. Metallurgical Transactions, 1973, 4B(12): 2679.
[17] Pickering F B. Physical Metallurgy and the Design of Steels [M]. London, UK: Applied Science Publishers, 1978.
[18] Dieter G E. Mechanical Metallurgy [M]. London, UK: McGraw-Hill Series in Materials Science and Engineering, 1981.
[19] Leslie W C. The Physical Metallurgy of Steels [M]. London, UK: McGraw-Hill International Book Company, 1981.
[20] Llewellyn D T. Steels: Metallurgy and Applications [M]. Oxford, UK: Butterworth-Heinemann Limited, 1992.
[21] Pero-Sanz J A. Steels: Physical Metallurgy. Selection and Design [M]. Madrid: CIE-Dossat 2000, 2004 (in Spanish).
[22] Hosford W F. Physical Metallurgy [M]. London: CRC Press, 2005.
[23] Pero-Sanz J A. Science and Materials Engineering [M]. Madrid: CIE-Dossat 2000, 2006 (in Spanish).
[24] Gawne D T, Lewis G M H. Strain Hardening of High Strength Steels [J]. Materials Science and Technology, 1985, 1(2): 128.
[25] Speich G R. Physical Metallurgy of Dual-Phase Steels [C]// Kot R A, Bramfitt B L. Fundamentals of Dual-Phase Steels. Pennsylvania, USA: The Metallurgical Society of AIME, 1981: 3.
[26] Verdeja J I, Busto A G, García J O, et al. Iron and Steel Making in the Third Millennium [J]. CIM Bulletin, 2006, 99 (1097): 1.
[27] Verdeja J I, Pero-Sanz J A, Asensio J. Multiphase Steels: Structure-Mechanical Properties Relationships in the Cold Rolled and Continuous Annealed Condition [C]// Rodriguez-Ibabe J M, Gutierrez I, López B, et al. Microalloying for New Steel Processes and Applications. Switzerland: Materials Science Forum, 2005: 429.